

# **Auto-Gopher-II – an autonomous wireline rotary-hammer ultrasonic drill**

Mircea Badescu, Hyeong Jae Lee, Stewart Sherrit, Xiaoqi Bao, Yoseph Bar-Cohen,  
Shannon Jackson, Jacob Chesin

**Jet Propulsion Laboratory, California Institute of Technology, (MS 67-119), 4800 Oak  
Grove Drive, Pasadena, CA 91109-8099, Phone 818-393-5700, Fax 818-393-2879,**

**Mircea.Badescu@jpl.nasa.gov** web: <http://ndea.jpl.nasa.gov>

and

Kris Zacny, and Gale L Paulsen

**Honeybee Robotics Spacecraft Mechanisms Corporation, Pasadena, CA**

**ABSTRACT** - Developing technologies that would enable future NASA exploration missions to penetrate deeper into the subsurface of planetary bodies for sample collection is of great importance. Performing these tasks while using minimal mass/volume systems and with low energy consumption is another set of requirements imposed on such technologies. A deep drill, called Auto-Gopher II, is currently being developed as a joint effort between JPL's NDEAA laboratory and Honeybee Robotics Corp. The Auto-Gopher II is a wireline rotary-hammer drill that combines formation breaking by hammering using an ultrasonic actuator and cuttings removal by rotating a fluted auger bit. The hammering mechanism is based on the Ultrasonic/Sonic Drill/Corer (USDC) mechanism that has been developed as an adaptable tool for many drilling and coring applications. The USDC uses an intermediate free-flying mass to transform high frequency vibrations of a piezoelectric transducer horn tip into sonic hammering of the drill bit. The USDC concept was used in a previous task to develop an Ultrasonic/Sonic Ice Gopher and then integrated into a rotary hammer device to develop the Auto-Gopher-I. The lessons learned from these developments are being integrated into the development of the Auto-Gopher-II, an autonomous deep wireline drill with integrated cuttings and sample management and drive electronics. Subsystems of the wireline drill are being developed in parallel at JPL and Honeybee Robotics Ltd. This paper presents the development efforts of the piezoelectric actuator, cuttings removal and retention flutes and drive electronics.

**KEYWORDS:** Life detection, planetary sampling, corer, wireline drill, piezoelectric devices.

## **1. INTRODUCTION**

A deep drill, called Auto-Gopher II, is currently being developed as a joint effort between JPL's NDEAA laboratory and Honeybee Robotics Corp. In the current configuration, the drill is being developed as both an ice drill, with potential application to deep drilling in the subsurface of Europa or Enceladus, and a regolith and soft rock drill, with potential application to Mars. The Auto-Gopher II is a wireline rotary-hammer drill that combines formation breaking by hammering using an ultrasonic actuator and cuttings removal by rotating a fluted auger bit. The hammering mechanism is based on the Ultrasonic/Sonic Drill/Corer (USDC) mechanism that has been developed as an adaptable tool for many drilling and coring applications [Bar-Cohen, 2001; Sherrit, 2000; Bao, 2003]. The USDC uses an intermediate free-flying mass or striker to transform high frequency vibrations of a piezoelectric transducer horn tip into sonic hammering of the drill bit. The USDC concept was used in a previous task to develop an Ultrasonic/Sonic Ice Gopher [Badescu, 2006] and then integrated into a rotary hammer device to develop the Auto-Gopher-I [Badescu, 2011, Bar-Cohen and Zacny, 2009]. The lessons learned from these developments are being integrated into the development of the Auto-Gopher-II, an autonomous deep wireline drill with integrated cuttings and sample management and drive electronics.

In developing the Auto-Gopher, the authors are seeking to demonstrate a scalable technology that makes deep drilling possible in the next two decades with current launch vehicles and power sources. The drill was demonstrated to reach 3 m in a 40MPa compressive strength gypsum formation, utilizing a wireline approach [Zacny et al., 2013]. The technology and concept of operation have been developed in conjunction with future mission constraints including mass, power and operation effectiveness. In the wireline approach, the drill is essentially a cylinder that includes a bit, drive mechanisms, actuators, and an anchor. The drill is suspended at the end of a lightweight tether and the

penetration depth is limited only by the packaging capability of the tether. This enables drilling to greater depths without a significant increase in system mass or complexity.

One of the limitations for drilling in planetary bodies is the available power. Proven power sources for landed missions are solar panels and Radioisotope Thermal Generators (RTG). In order for the Auto-Gopher to drill through ice, a few 100 Watt of power can result in 10-20 minutes of drilling per hour (based on 300 W drilling consumption). In contrast, an ice melt probe would require kW's of power and this requires development of small, space-worthy nuclear reactor, which will be very expensive and take a long time to develop. One of the drawbacks of the wireline system is the possibility of borehole collapse. To deal with that, the drill could come with deployable (e.g. mesh type) casings but the complexity of deploying a casing would currently make the missions prohibitively risky. For this reason, the drilled environment should be restricted to stable formations such as ice or ice-cemented grounds, where the probability of finding life would be highest. In turn, plausible targets would include the Northern and the Southern Polar Regions of Mars, or Enceladus, and Europa.

Subsystems of the Auto-Gopher II wireline drill are being developed in parallel at JPL and Honeybee Robotics Ltd. This paper presents the development efforts of the piezoelectric actuator, cuttings removal and retention flutes and drive electronics.

## 2. PIEZOELECTRIC ACTUATOR DEVELOPMENT

In parallel to the core break-off mechanism development, we investigated a smaller scale actuator which was able to provide 100W power and use the bus voltage provided for the whole drill. The selection was made to develop an actuator that uses 6.35mm (0.25") thick PZT disks that would work at the 360V provided by the drill bus. The voltage level was selected based on reduction of the power loss for a 1000 m long cable.

### 2.1 10kHz piezoelectric transducer development

The piezoelectric actuator transducer includes a piezoelectric stack with 8 PZT8 active rings and two passive rings, one at each end of the stack to allow the ground to be isolated from the metal of the drill. A titanium (TI-6Al-4V) stepped dog-bone horn amplifies the vibrations displacement of the piezoelectric stack. The PZT rings in the stack are held in compression between the horn base and a backing using a pre-stress bolt. A solid model of the piezoelectric actuator was generated and it is shown in Figure 1. An FEA model of the piezoelectric transducer was generated using Ansys™ (Figure 2). In this model uses the actuator geometric parameters (such as the length of the piezoelectric stack, the backing, and the horn) were adjusted to obtain a piezoelectric transducer with a resonant frequency of about 10kHz. The neutral plane was designed to be located inside the horn base and away from the horn – piezoelectric disks interface. The design and the geometric parameters are shown in Figure 3 and the materials and their characteristics are shown in Table 1

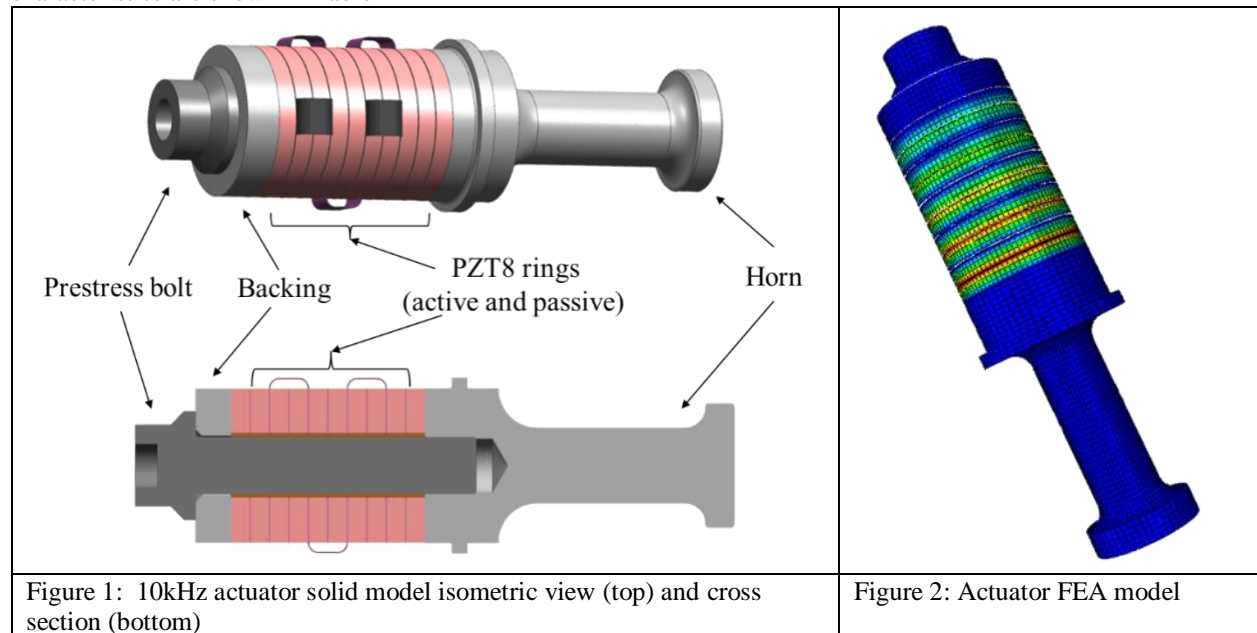


Table 1: Actuator materials

	OD (mm)	ID (mm)	Length (mm)	Young's modulus (GPa)	$\rho$ (kg/m <sup>3</sup> )	Poisson's ratio	$\sigma_c$ (MPa)
Piezo (PZT8)	50.8	21.6	6.35	-	7500	0.3	517 (35)
Backing (Steel)	50.8	18.76	12	205	7850	0.28	250
Horn (Titanium)	-	-	68	116	4506	0.34	970 (880)

The actuator was assembled and the impedance spectrum was measured and analyzed. Modal analysis of the piezoelectric transducer was performed in order to identify the mode shapes and natural frequencies of the chosen piezoelectric actuator design. The actuator shown in Figure 3 has a resonance frequency of 10 kHz and a Q factor of 100 at low signal.

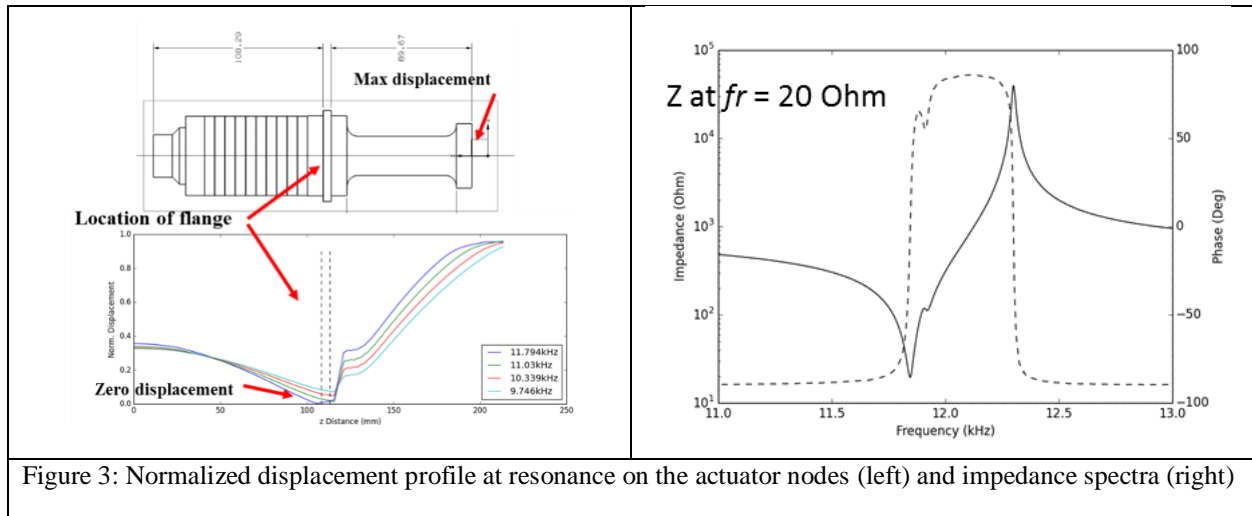


Figure 3: Normalized displacement profile at resonance on the actuator nodes (left) and impedance spectra (right)

After parts fabrication and actuator assembly the impedance spectra of the actuator was then re-measured and the actuator was integrated into a testbed. The goal of the testbed was to determine the maximum kinetic energy the striker can acquire after the impact with the transducer horn tip and the frequency of the impact. The testbed design and fabricated hardware are shown in Figure 4. The testbed includes a vertically mounted plate where the actuator is mounted at the neutral plane flange. The actuator is mounted with the horn tip facing up to eliminate the need of a striker preload spring. A solid rod was used as a bit replacement and was mounted between two high stiffness wave springs preloaded between two plate-mounted collars. The gap between the bit replacement and the striker could be adjusted to determine an optimal value where the striker reaches resonance.

## 2.2 5kHz piezoelectric actuator development

The size of the bit diameter and the teeth contact area suggest that the striker impact energy be larger than 1J. Preliminary testing with the 10 kHz actuator showed striker impact energy smaller than the desired minimum value and a decision was made to redesign the actuator to have larger horn tip displacement and this required a larger piezoelectric stack. The redesigned actuator has additional alumina disks that insulate electrically the piezoelectric stack electrodes from the transducer horn, backing and stress bolt allowing the ground to float. The actuator solid model is shown in Figure 6 and a hardware implementation without the insulating alumina disks is shown integrated into the impact testbed in Figure 5.

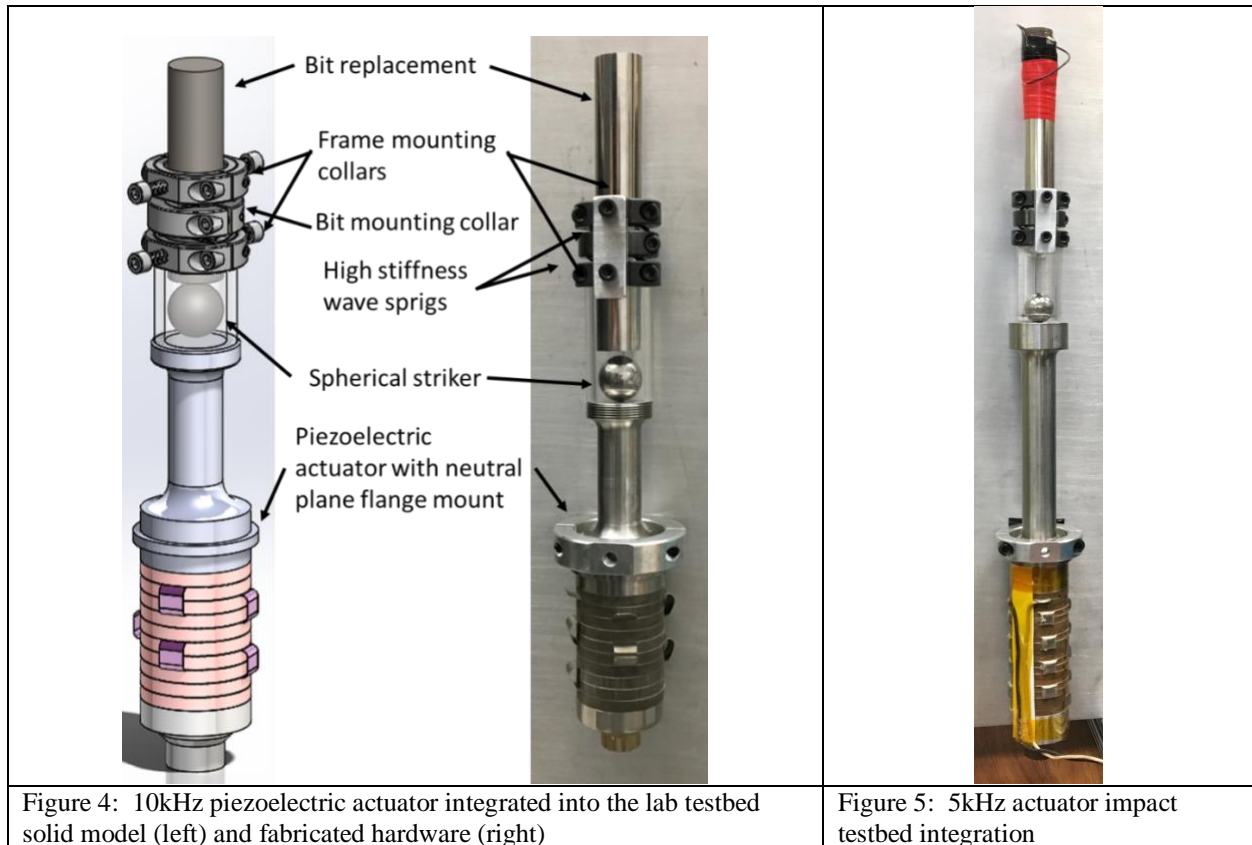


Figure 4: 10kHz piezoelectric actuator integrated into the lab testbed solid model (left) and fabricated hardware (right)

Figure 5: 5kHz actuator impact testbed integration

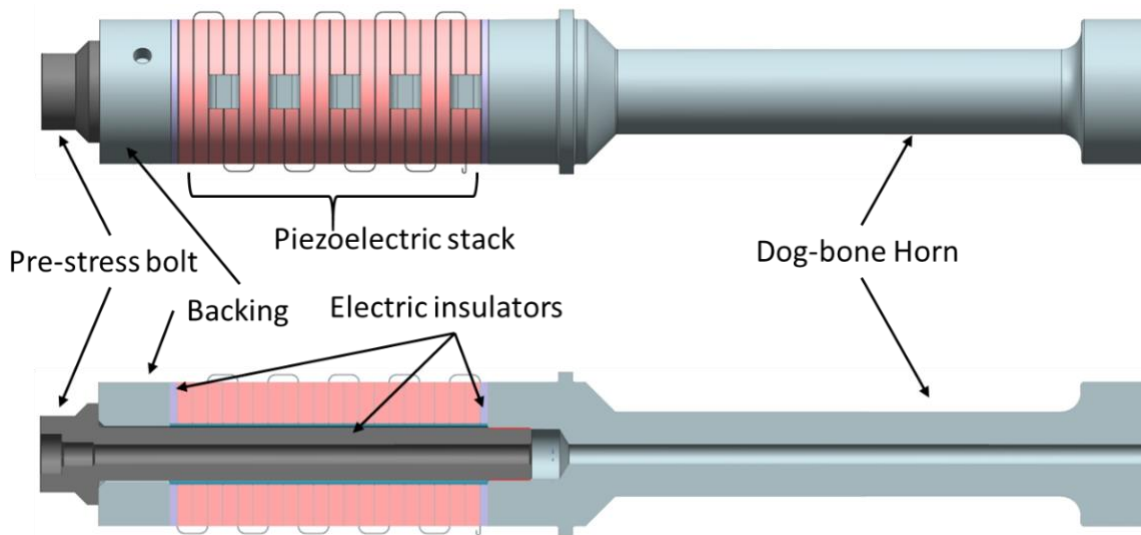


Figure 6: The piezoelectric actuator side view (top) and cross section (bottom)

### 3. CUTTINGS REMOVAL TESTING

The auger section of the drill bit has two main purposes: collect the cuttings from the drill bit head and retain them when the drill is brought to the surface and removed from the hole. 3D printed helical screw blade of the auger were investigated to test the ability to hold the cuttings on the flutes without jamming. The material used was PLA (PolyLactic Acid) thermoset polymers. The entire drill unit was assembled using a custom made drill bit head, PLA 3D printed adapter, PLA 3D printed helical screw blade with hollow center, and a steel rod (Figure 7). A drilling testbed was assembled (Figure 8) consisting of aluminum T-slot framing, a linear bearing, and a commercial hammering drill. The linear motion is controlled using a pulley system with counter weight to allow varying the

applied weight on bit. In order to simulate the auger removing sample material from a hole, a Plexiglas tube with a diameter slightly larger than that of the auger was filled with sand. This approach was selected because, in-situ, the drill creates a hole similar to the inner diameter of the pipe in the hard surface being drilled. This setup allows the drill to run with the auger while varying the drill speed and applied weight on bit. Optimal results with this setup (i.e. maximum material removal/retention by the auger) were found to be  $\sim 32\text{N}$  force and 100-150 RPM. Once the auger is approximately 80% submerged into the pipe, the drill is stopped and pulled from the hole in order to retrieve and evaluate the sample material from the hole (Figure 9).

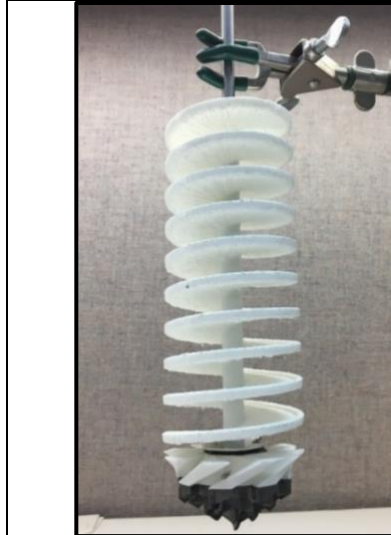


Figure 7: Assembled drill bit unit

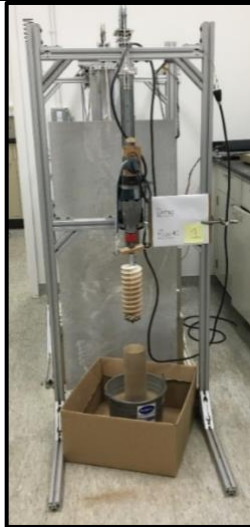


Figure 8: Testbed overall view (left) and close-up (right)

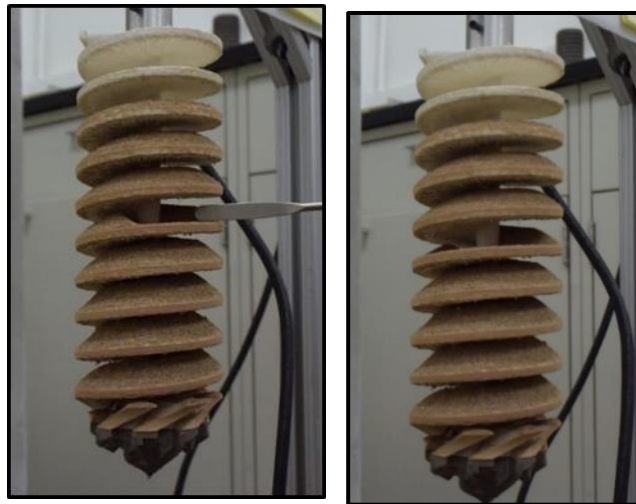


Figure 9: drill bit flutes showing the profile of the removed sand.

#### 4. ELECTRONICS DRIVER DEVELOPMENT

The goals for the electronics component of our task is to develop an electronic driver, enable use of the bus drive voltage, work at temperatures of  $100^{\circ}\text{C}$  or less and fits in the space allocated inside the drill body. This effort led to the development of firmware to test the drive of the actuators and to explore packaging possibilities. The focus has been on completing the entire electronics design including wiring interfaces with acceptable isolation, connectors and high speed fusing of the high voltage. One lab test of the driver was performed with a vertically mounted 5kHz piezoelectric transducer and a ball bearing spherical striker with good results. During one of the tests, while running with 100 watts of power, the free-mass ball was lifted over 6-inches completely out of its retaining tube. However, this test also had uncovered a shortcoming in the drive electronics - the resolution of the 50Hz frequency steps

produced by the micro-controller were not sufficiently enough to fine-tune the resonance. Therefore, a programmable oscillator using a DAC and VCO was implemented which now gives the driver frequency steps down to 1Hz.

Because of the long 100-meter-high voltage feed line from the surface and the unique current waveforms of the driver output, a realistic power line test was performed (Figure 10). There was a concern that the electronics might become unstable or impose excessive noise on the main electronics system. In order to test this, the high voltage of our drive electronics was driven with 100 Meters of 16 gauge twisted pair cable. 300VDC was used at the input to the cable while driving the piezoelectric actuator up to 150W RMS. The driver was found to be stable, with less than 2V p-p observed at the output of the cable and only 150mV p-p at the power source

As part of the design, we require the isolation of the piezoelectric stack from the chassis ground and fast fusing to prevent a malfunction in the piezoelectric driver from pulling down the main system's high voltage. A circuit design solution for fast resettable fusing of the high voltage line was done (Figure 11). Trip current level, breaker resetting and status can be managed over the RS485. The 28V line has a resettable Poly Fuse while the Phillips Driver IC uses a standard fuse.

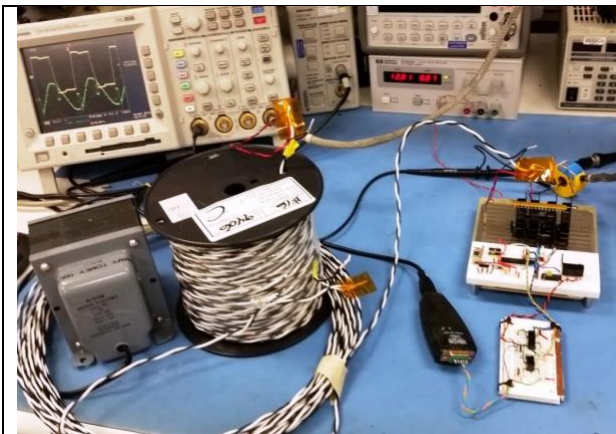


Figure 10: Test of the signal strength with 100-meter cable.

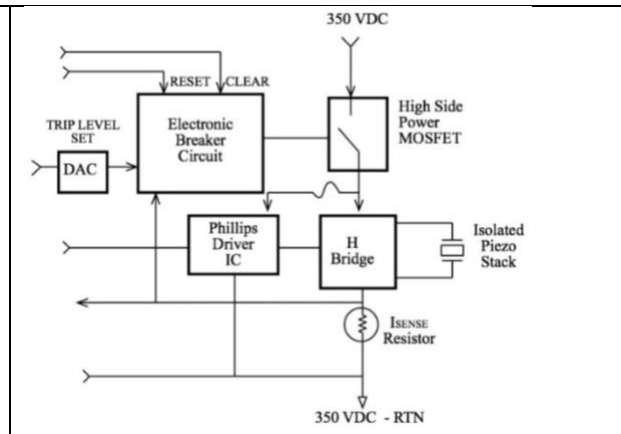


Figure 11: Block diagram of circuit design I – high voltage electronic circuit breaker.

A RS485 communication scheme using Modbus protocol, rather than Ethernet, was agreed upon with the development team of the drill system at Honeybee. Since the driver operation is somewhat autonomous, instrument commands and data transfers require low bandwidth. The piezoelectric driver electronics is treated by the larger system more like a motor/sensor and less like a CPU. The RS485 communications, along with the main system's 28V supply, has been completely electrically isolated from the high voltage driver electronics (Figure 12). To achieve the highest common mode isolation and safety, slotted optical switches rather than typical opto-isolators are used. A 105°C capable 28V to 9V DC-to-DC convertor with a post wide band voltage regulator will be used for the first PCB. A simplified Block Diagram with the correct interface was designed and it is shown in Figure 13.

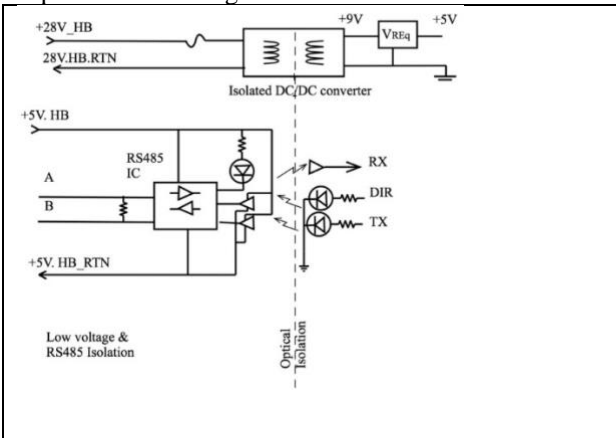


Figure 12: Block diagram of circuit design II – low voltage and RS485 isolation.

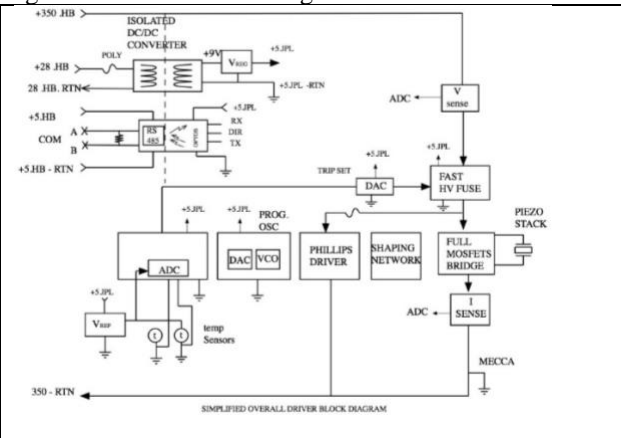


Figure 13: Simplified overall driver block diagram

All required power, communication and sensor connectors have been chosen by Honeybee Robotics. The connectors mount on our metal enclosure and are of the pig-tailed wire variety simplifying this phase of the design (Figure 14). An approximate conservative PCB parts layout is continually updated in order to keep track of the size of the electronics PCB design and not to be surprised later in the project. This is a 4-layer board with minimal parts on the back plane and can be reduced in size if necessary.

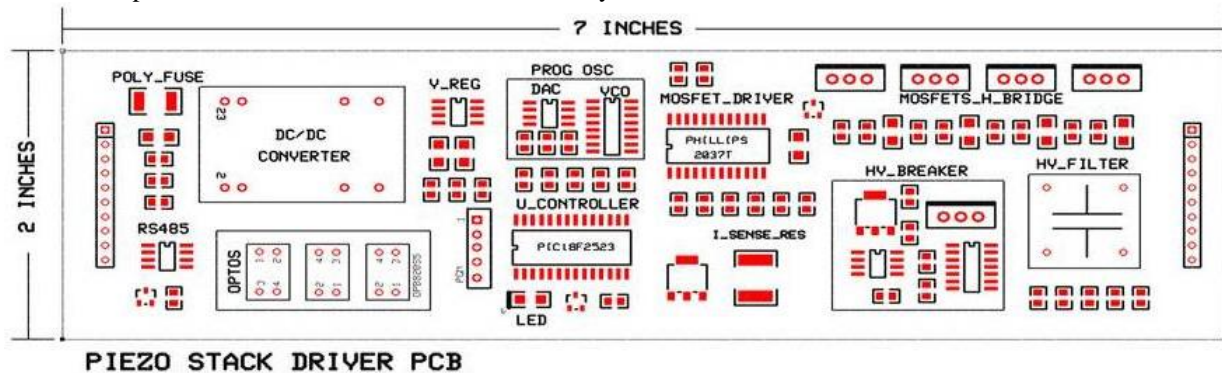


Figure 14: Schematic of PCB parts layout

### 5. PIEZOELECTRIC ACTUATOR BIT INTEGRATION

In the next development step, we will assemble the electrically isolated piezoelectric transducer and integrate it with the drill bit (Figure 15). The drill bit includes a hollow bit stem with a helical screw blade (flutes) connected to the full-face drill bit head using a flexure. The bit stem is connected to the rotary section of the drill. The flexure has a low axial stiffness but can transfer torque to the drill bit head. Inside the hollow bit stem there is an anvil that has high axial rigidity, which will be used to transfer the striker impacts directly to the drill bit head. The low axial stiffness flexure acts as an impact isolator allowing the impact energy of the striker to be transferred to the drill bit head only and not to the bit stem.

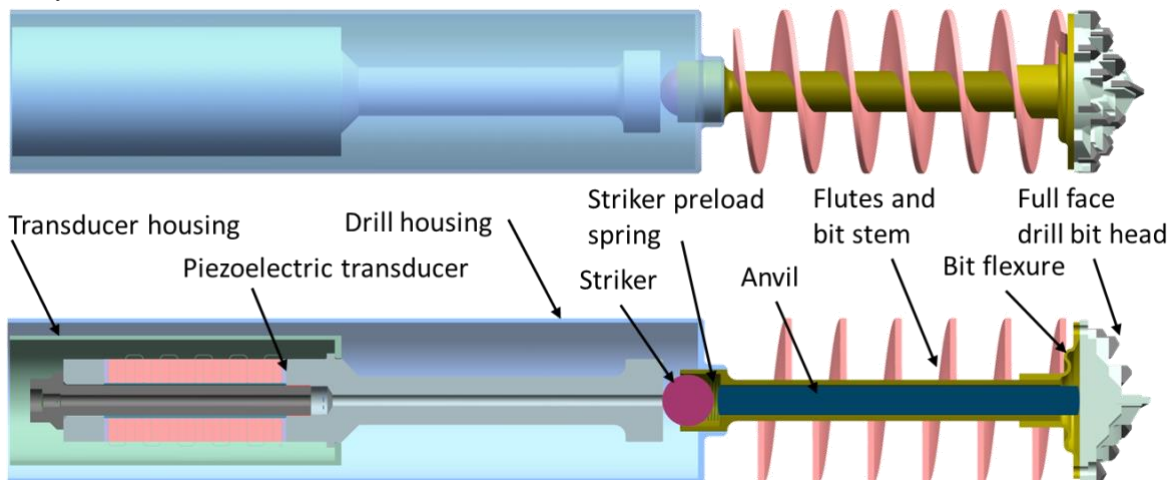


Figure 15: Integrated piezoelectric actuator, striker, anvil, bit head, bit flexure, flutes and bit stem

### 6. Conclusions and future work

In this paper, we presented the current state of development of the piezoelectric transducer for the Auto\_Gopher-II, including the drive electronics, and integration with an auger drill bit. Testing of the initial 10 kHz transducer suggested that the momentum transfer to the free mass was not sufficient to produce fracture stress at the rock bit interface. The testing on a modified 5 kHz transducer however found impact energies at the 1 J level. In addition, we developed an augering bit, which allowed for hammering action on the teeth of the bit but did not transmit significant forces to the flutes of the auger.

We will continue fabricating the proposed drill bit configuration, integrate it with the transducer and test with the developed drive electronics. After preliminary tests completion the hardware and drive electronics will be integrated into the drill system at Honeybee Robotics, Ltd.

### Acknowledgements

Research reported in this abstract was conducted at the Jet Propulsion Laboratory (JPL), California Institute of Technology, jointly with Honeybee Robotics under a contract with National Aeronautics Space Administration (NASA). This research is funded by the NASA's MatISSE (Maturation of Instruments for Solar System Exploration) program.

### References

- [1] Aldrich J.B., S. Sherrit, Y. Bar-Cohen, X. Bao, M. Badescu, and Z. Chang. "Extremum-seeking control of Ultra-sonic/Sonic Driller/Corer (USDC) driven at high-power", Proceedings of the SPIE Modeling, Signal Processing and Control Conf., Volume 6166 (2006b).
- [2] Badescu, M., Sherrit, S., Olorunsola, A.K., Aldrich, J., Bao, X., Bar-Cohen, Y., Chang, Z., Doran, P.T., Kenig, F., Fritsen, C., Murray, A., McKay, CP., Peterson, T., Du, S., Tao, S., "Ultrasonic/Sonic Gopher for Subsurface Ice and Brine Sampling: Analysis and Fabrication Challenges, and Testing Results", Proceedings of the SPIE 13th Annual Symposium on Smart Structures and Materials, San Diego, CA, SPIE Vol. 6171-07, 26 February – 2 March, 2006.
- [3] Badescu, M., Kassab, S., Sherrit, S., Aldrich, J., Bao, X., Bar-Cohen, Y., and Chang, Z. (2007). "Ultrasonic/Sonic Driller/Corer as a hammer-rotary drill." Proc., of the 14th International Symposium on: Smart Structures and Materials & Nondestructive Evaluation and Health Monitoring, International Society for Optics and Photonics, 65290S.
- [4] Badescu, M., Sherrit, S., Bao, X., Bar-Cohen, Y., Chen, B., "Auto-Gopher - a wire-line rotary-hammer ultrasonic drill," Proceedings of the SPIE International Symposium on Smart Structures and Nondestructive Evaluation, SPIE SS11-SSN07-157 7981-135, San Diego, CA, 6-10 March, 2011.
- [5] Bao, X., Bar-Cohen, Y., Chang, Z., Dolgin, B. P., Sherrit, S., Pal, D. S., Du, S., and Peterson, T. (2003). "Modeling and computer simulation of ultrasonic/sonic driller/corer (USDC)." *Ultrasonics, Ferroelectrics and Frequency Control*, IEEE Transactions on, 50(9), 1147-1160.
- [6] Bar-Cohen, Y., Sherrit, S., Dolgin, B., Bao, X., Chang, Z., Krahe, R., Kroh, J., Pal, D., Du, S., Peterson, T., "Ultrasonic/Sonic Driller/Corer (USDC) for planetary application," Proc. SPIE Smart Structure and Materials 2001, pp. 529-551, 2001.
- [7] Bar-Cohen Y., S. Sherrit, X. Bao, M. Badescu, J. Aldrich and Z. Chang, "Subsurface Sampler and Sensors Platform Using the Ultrasonic/Sonic Driller/Corer (USDC)," Paper #6529-18, SPIE Smart Structures and Materials Symposium, San Diego, CA, March 19-22, 2007
- [8] Bar-Cohen, Y., and Zacny, K. (2009). *Drilling in extreme environments: penetration and sampling on earth and other planets*, John Wiley & Sons.
- [9] NASA Astrobiology Website Roadmap <http://astrobiology.arc.nasa.gov/roadmap>
- [10] Navarro-Gonzalez, R., F. A. Rainey, P. Molina, D. R. Bagaley, B. J. Hollen, J. de la Rosa, A. M. Small, R. C. Quinn, F. J. Grunthaner, L. Caceres, B. Gomez-Silva and C. P. McKay (2003). Mars-like soils in the Atacama Desert, Chile, and the dry limit of microbial life. *Science* 302 (5647): 1018-1021.
- [11] *New Frontiers in the Solar System: An Integrated Exploration Strategy*; Solar System Exploration Survey, National Research Council, Washington, DC (2003).
- [12] S. Sherrit, X. Bao, Z. Chang, B. Dolgin, Y. Bar-Cohen, D. Pal, J. Kroh, T. Peterson "Modeling of the ultrasonic/sonic driller/corer: USDC," 2000 IEEE Int. Ultrason. Symp. Proc., vol.1, pp. 691-694, 2000.
- [13] Zacny, K., G. Paulsen, B. Mellerowicz, Y. Bar-Cohen, L. Beegle, S. Sherrit, M. Badescu, F. Corsetti, J. Craft, Y. Ibarra, X. Bao, and H. J. Lee, *Wireline Deep Drill for Exploration of Mars, Europa, and Enceladus*, 2013 IEEE Aerospace Conference, Big Sky, Montana, March 2-9, 2013.
- [14] Zacny, K., Y. Bar-Cohen, M. Brennan, G. Briggs, G. Cooper, K. Davis, B. Dolgin, D. Glaser, B. Glass, S. Gorevan, J. Guerrero, C. McKay, G. Paulsen, S. Stanley, and C. Stoker, *Drilling Systems for Extraterrestrial Subsurface Exploration*, *Astrobiology Journal*, Volume 8, Number 3, 2008, DOI: 10.1089/ast.2007.0179